



Synthesis and hydration behavior of calcium zirconium aluminate ($\text{Ca}_7\text{ZrAl}_6\text{O}_{18}$) cement



Eun-Hee Kang^a, Jun-Sang Yoo^b, Bo-Hye Kim^a, Sung-Woo Choi^a, Seong-Hyeon Hong^{a,*}

^a Department of Materials Science and Engineering, Research Institute of Advanced Materials, Seoul National University, Seoul 151-744, South Korea

^b Department of Oral & Maxillofacial Surgery, School of Dentistry, Seoul National University, Seoul 110-749, South Korea

ARTICLE INFO

Article history:

Received 26 November 2012

Accepted 14 November 2013

Keywords:

Calcium zirconium aluminate

Calcium aluminate cement (D)

Hydration (A)

Microstructure (B)

ABSTRACT

Calcium zirconium aluminate ($\text{Ca}_7\text{ZrAl}_6\text{O}_{18}$) cements were prepared by solid state reaction and polymeric precursor methods, and their phase evolution, morphology, and hydration behavior were investigated. In polymeric precursor method, a nearly single phase $\text{Ca}_7\text{ZrAl}_6\text{O}_{18}$ was obtained at relatively lower temperature (1200 °C) whereas in solid state reaction, a small amount of CaZrO_3 coexisted with $\text{Ca}_7\text{ZrAl}_6\text{O}_{18}$ even at higher temperature (1400 °C). Unexpectedly, $\text{Ca}_7\text{ZrAl}_6\text{O}_{18}$ synthesized by polymeric precursor process was the large-sized and rough-shaped powder. The planetary ball milling was employed to control the particle size and shape. The hydration behavior of $\text{Ca}_7\text{ZrAl}_6\text{O}_{18}$ was similar to that of $\text{Ca}_3\text{Al}_2\text{O}_6$ (C3A), but the hydration products were $\text{Ca}_3\text{Al}_2\text{O}_6 \cdot 6\text{H}_2\text{O}$ (C3AH6) and several intermediate products. Thus, Zr (or ZrO_2) stabilized the intermediate hydration products of C3A.

© 2013 Elsevier Ltd. All rights reserved.

1. Introduction

In dentistry, calcium silicate-based cements are used for dental root canal filling and repair materials, but their radiopacity is not sufficient to be visualized radiographically [1–4]. To distinguish the filling and repair materials from the surrounding anatomical structures (dentine), radiopacifying materials such as bismuth oxide, zinc oxide, and zirconium oxide has to be added to the calcium silicate-based cements [1,5,6]. However, the addition of a radiopacifier in a minimal amount can change the setting chemistry, biocompatibility, and physical properties of the cements. In this aspect, it is beneficial to develop the cement with the radiopacifier as a component instead of as an additive, and ZrO_2 -containing calcium aluminate ($\text{Ca}_7\text{ZrAl}_6\text{O}_{18}$) cement is a promising candidate.

$\text{Ca}_7\text{ZrAl}_6\text{O}_{18}$ is only a compound with hydration reactivity in $\text{CaO-Al}_2\text{O}_3\text{-ZrO}_2$ system [7–9]. Its crystal structure is orthorhombic with a space group of $\text{Pmn}2_1$, in which five types of Ca atoms and four types of AlO_4 tetrahedra are positionally and orientationally disordered, respectively [9]. The hydration behavior of $\text{Ca}_7\text{ZrAl}_6\text{O}_{18}$ is comparable to that of $\text{Ca}_3\text{Al}_2\text{O}_6$ (C3A), and $\text{Ca}_7\text{ZrAl}_6\text{O}_{18}$ is free from premature setting. $\text{Ca}_7\text{ZrAl}_6\text{O}_{18}$ is expected to take the place of $\text{Ca}_3\text{Al}_2\text{O}_6$ in normal Portland cement and have a potential application as dental root canal filling and repair materials, but the studies were very limited and very few reports have been published [7–10].

$\text{Ca}_7\text{ZrAl}_6\text{O}_{18}$ has been synthesized by a conventional solid state reaction [7,9], which requires a high temperature and a prolonged sintering time. Polymeric precursor (or Pechini) method is a low temperature

sol-gel route based on the polybasic acids (e.g., citric acid) to form chelates with metallic ions. The chelates undergo polyesterification upon heating with the polyhydroxyl alcohols (e.g., ethylene glycol) to form the large metal-organic complexes [11,12]. This method offers a molecular level mixing resulting in the powders with a high purity, an ultrahigh homogeneity, a wide range of particle size, and a lower calcination temperature. The polymeric precursor method has been employed to prepare the calcium aluminate and calcium silicate cements [13–15], but it has not been applied to synthesize the $\text{Ca}_7\text{ZrAl}_6\text{O}_{18}$ cement.

In this study, calcium zirconium aluminate ($\text{Ca}_7\text{ZrAl}_6\text{O}_{18}$) was synthesized by polymeric precursor and solid-state reaction methods, and their phase evolution and morphology were investigated. The synthesized $\text{Ca}_7\text{ZrAl}_6\text{O}_{18}$ powder was treated by planetary ball milling to control the particle size and morphology. In addition, the hydration behavior and radiopacity of $\text{Ca}_7\text{ZrAl}_6\text{O}_{18}$ were examined and compared with that of $\text{Ca}_3\text{Al}_2\text{O}_6$ (C3A), which was prepared in the similar manner.

2. Materials and methods

For solid state reaction synthesis, the stoichiometric mixture of CaCO_3 (Acros, Geel, Belgium), ZrO_2 (Fine Materials, Korea), and Al_2O_3 (Aldrich, Milwaukee, WI) was mixed in acetone, ball milled for 24 h, and then dried in an oven for 24 h. The dried mixtures were pre-calcined at 900 °C for 3 h in air and then annealed at 1000–1400 °C for 3 h. In polymeric precursor process, $\text{Ca}(\text{NO}_3)_2 \cdot 4\text{H}_2\text{O}$ (Aldrich, Milwaukee, WI), $\text{ZrO}(\text{NO}_3)_2$ (Aldrich, Milwaukee, WI), and $\text{Al}(\text{NO}_3)_3 \cdot 9\text{H}_2\text{O}$ (Aldrich, Milwaukee, WI) were used as starting materials. The resin was composed of 60 wt.% citric acid monohydrate and 40 wt.% ethylene glycol, and the resin content was fixed at 85 wt.% of the oxide weight. The

* Corresponding author. Tel.: +82 28806273; fax: +82 28841413.
E-mail address: shhong@snu.ac.kr (S.-H. Hong).

mixed solution was heated to evaporate the water and charred at 250 °C for 3 h. The resulting gels were finely ground and then calcined at 750 °C for 3 h. The calcined powders were annealed at 1300–1600 °C for 3 h in air. For comparison, $\text{Ca}_3\text{Al}_2\text{O}_6$ (C3A) was prepared by polymeric precursor process using $\text{Ca}(\text{NO}_3)_2 \cdot 4\text{H}_2\text{O}$ and $\text{Al}(\text{NO}_3)_3 \cdot 9\text{H}_2\text{O}$, and the annealing was conducted at 1200 °C for 3 h. To reduce the particle size, as-calcined powders (at 900 °C) were ground by planetary ball mill with zirconia balls and zirconia jar in absolute ethanol medium. The rotation speed was 250 rpm and milling time was 1 h. The milled powders were dried at 80 °C for 24 h and then annealed at 1200 °C for 3 h.

For the hydration studies, annealed powders ($\text{Ca}_7\text{ZrAl}_6\text{O}_{18}$ and $\text{Ca}_3\text{Al}_2\text{O}_6$) were mixed with distilled water, and pastes were cast into plastic vials. The water to cement ratio (w/c) was fixed at 1.0 for all samples. The vials were stored in a sealed container containing water and demolded after fixed times (1 min–7 days). The hydration was stopped by immersing the crushed samples in methanol for 3 days, and the methanol exchanged samples were dried in a N_2 atmosphere.

The phases of annealed and hydrated samples were examined by X-ray diffraction (XRD, D8-Advance, BRUKER MILLER Co.) using $\text{Cu K}\alpha$ radiation ($\lambda = 1.5406 \text{ \AA}$). The morphology of the powders was observed by field emission scanning electron microscopy (FE-SEM, JSM-7401 F, JEOL). The semi-quantitative elemental composition was determined by energy dispersive X-ray spectroscopy (EDS) at an acceleration voltage of 15 kV using an ISIS 300 system (Link Analytical, Oxford Instruments). The specific surface area of the annealed powders was measured using nitrogen absorption (BET, Model ASAP 2010, Micromeritics Instrument Corp., Norcross, GA). The temperature changes during hydration were measured by inserting the conventional probe type digital thermometer in the pastes. For a radiopacity evaluation, the specimens ($\text{Ca}_7\text{ZrAl}_6\text{O}_{18}$ and $\text{Ca}_3\text{Al}_2\text{O}_6$) were cured at 37 °C for 28 days. The specimens were placed directly on a phosphor imaging plate adjacent to a calibrated aluminum step hole with 3 mm thickness. A standard X-ray machine (GEC Medical Equipment Ltd., Middlesex, UK) was used to irradiate X-rays onto the specimens using an exposure time of 0.48 s at 10 mA at a cathode-target film distance of $300 \pm 10 \text{ mm}$. The tube voltage was set at $65 \pm 5 \text{ kV}$. The radiographs were processed in an automatic processing machine (Clarimat 300, Gendex Dental Systems, Medivance Instruments Ltd., London, UK) and a digital image of the radiograph was obtained.

3. Results and discussion

3.1. Phase and morphology

The XRD patterns for $\text{Ca}_7\text{ZrAl}_6\text{O}_{18}$ powders prepared by solid-state reaction are shown in Fig. 1 as a function of annealing temperature. At 1000 °C, CaZrO_3 and $\text{Ca}_3\text{Al}_2\text{O}_6$ (C3A) were formed, but unreacted starting materials (CaO , ZrO_2 , and Al_2O_3) were still observed (Fig. 1(A)). With increasing the annealing temperature, the peak intensity for CaZrO_3 and C3A increased with the expense of starting materials (Fig. 1(B), (C)). At 1300 °C, these two phases were transformed into $\text{Ca}_7\text{ZrAl}_6\text{O}_{18}$ with a small amount of CaZrO_3 (Fig. 1(D)). According to the intensity ratio of XRD main peaks ($I_{\text{CaZrO}_3}/I_{\text{Ca}_7\text{ZrAl}_6\text{O}_{18}}$), the amount of CaZrO_3 secondary phase was estimated to be $\sim 2.6\%$. The obtained diffraction pattern of $\text{Ca}_7\text{ZrAl}_6\text{O}_{18}$ was well matched with the previous pattern based on the orthorhombic crystal structure with a space group of Pmmn_2_1 [9]. However, CaZrO_2 could not be eliminated even at higher temperature (Fig. 1(E)) or for a longer annealing time.

In polymeric precursor method, $\text{Ca}_7\text{ZrAl}_6\text{O}_{18}$ was obtained at as low as 1000 °C although the peaks were broad and the peak intensity was weak (Fig. 2(A)). No intermediate secondary phases such as $\text{Ca}_3\text{Al}_2\text{O}_6$, $\text{Ca}_5\text{Al}_6\text{O}_{14}$, and $\text{Ca}_{12}\text{Al}_{14}\text{O}_{33}$ were observed [8,16]. With the increase of annealing temperature, the peak intensity for $\text{Ca}_7\text{ZrAl}_6\text{O}_{18}$ increased and the diffraction peaks were well separated indicating the enhanced crystallinity (Fig. 2(B), (C)). No difference was found in the XRD

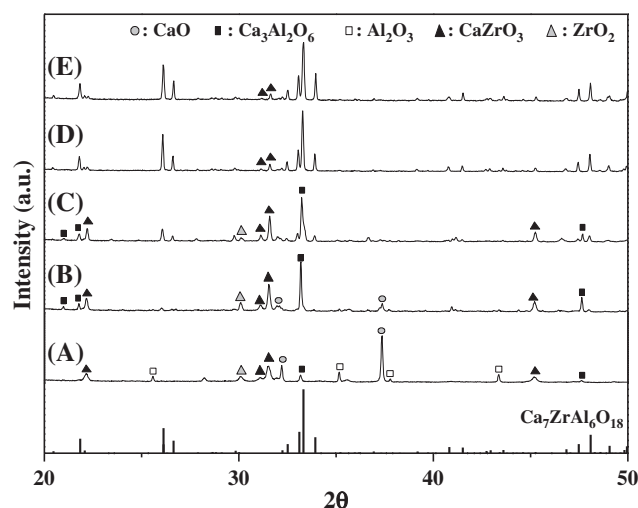


Fig. 1. X-ray diffraction patterns of $\text{Ca}_7\text{ZrAl}_6\text{O}_{18}$ synthesized by solid-state reaction as a function of annealing temperature; (A) 1000, (B) 1100, (C) 1200, (D) 1300, and (E) 1400 °C.

patterns of the powders annealed at 1300 and 1400 °C (Fig. 2(D), (E)) and thus, the annealing temperature was fixed at 1200 °C for the subsequent studies. Consequently, the polymeric precursor method was very effective to synthesize the $\text{Ca}_7\text{ZrAl}_6\text{O}_{18}$ phase at the relatively low temperature. In all the powders prepared by polymeric precursor process, a minor amount of CaZrO_2 ($\sim 0.9\%$) was present, and a single phase of $\text{Ca}_7\text{ZrAl}_6\text{O}_{18}$ was realized when the less amount of $\text{ZrO}(\text{NO}_3)_2$ than the stoichiometric ratio (≤ 0.95) was used (see the Supplementary data Fig. S1a). The lattice parameter of single phase $\text{Ca}_7\text{ZrAl}_6\text{O}_{18}$ ($\text{ZrO}(\text{NO}_3)_2 = 0.9$) was determined by the Si internal standard method (see the Supplementary data Fig. S1b). The refined lattice parameters based on the orthorhombic crystal structure (Pmmn_2_1) were $a = 10.844(3)$, $b = 10.601(1)$, and $c = 7.669(1) \text{ \AA}$, which were well agreed with the reported data [9].

The morphology of a nearly single phase $\text{Ca}_7\text{ZrAl}_6\text{O}_{18}$ is shown in Fig. 3. The $\text{Ca}_7\text{ZrAl}_6\text{O}_{18}$ powder prepared by solid-state reaction at 1300 °C exhibited a rather round shape with a smooth surface, and the particle size was approximately $5 \mu\text{m}$ (Fig. 3(A)). Further increase of annealing temperature to 1400 °C caused the significant coarsening (or sintering) and resulted in the larger particle size. On the other hand, the powder synthesized by polymeric precursor process at

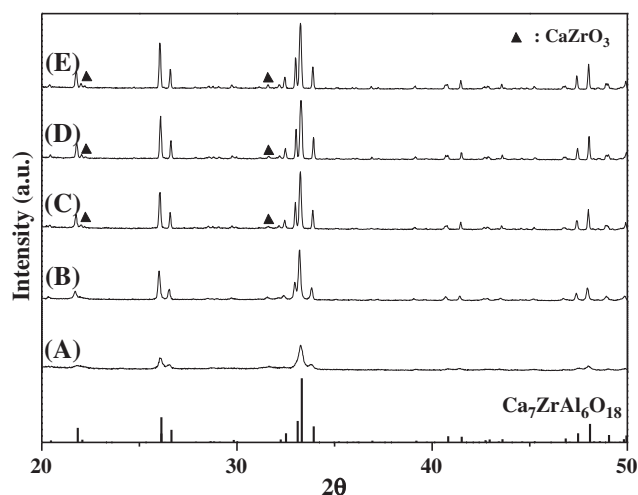


Fig. 2. X-ray diffraction patterns of $\text{Ca}_7\text{ZrAl}_6\text{O}_{18}$ synthesized by polymeric precursor process as a function of annealing temperature; (A) 1000, (B) 1100, (C) 1200, (D) 1300, and (E) 1400 °C.

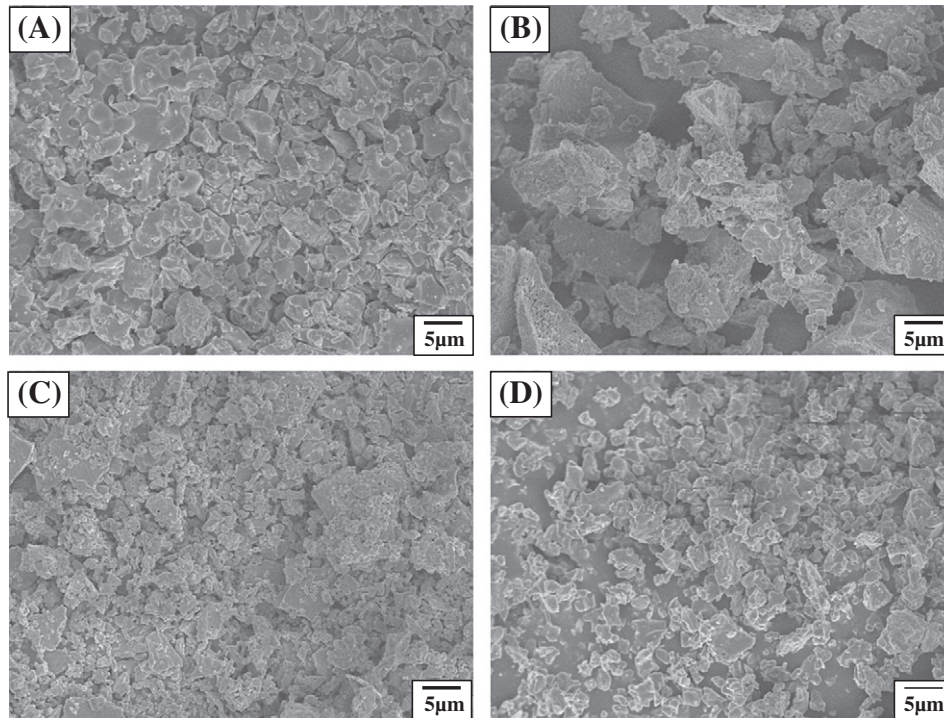


Fig. 3. FE-SEM images of $\text{Ca}_7\text{ZrAl}_6\text{O}_{18}$ synthesized by (A) solid state reaction at 1300 °C and (B) polymeric precursor process at 1200 °C. (C) $\text{Ca}_7\text{ZrAl}_6\text{O}_{18}$ prepared by polymeric precursor process and planetary ball milling and (D) C3A prepared by polymeric precursor process at 1200 °C.

1200 °C showed the rough and irregular fracture morphology with an inhomogeneous size distribution (Fig. 3(B)). This was unexpected because the polymeric precursor process commonly produces the very fine, homogeneous, and spherical powders [17,18]. To reduce the particle size and size distribution, the powder calcined at 900 °C was ground by planetary ball milling and annealed at 1200 °C. The formation of $\text{Ca}_7\text{ZrAl}_6\text{O}_{18}$ was examined by XRD and the size reduction was confirmed by SEM (Fig. 3(C)). Consistent with SEM observation, the specific surface area increased from 0.7 to 1.7 m^2/g after milling. It is expected that the size of $\text{Ca}_7\text{ZrAl}_6\text{O}_{18}$ powder can be further reduced after a prolonged milling time. To compare the hydration behavior of

$\text{Ca}_7\text{ZrAl}_6\text{O}_{18}$ with that of $\text{Ca}_3\text{Al}_2\text{O}_6$ (C3A), C3A was synthesized in the same way using the polymeric precursor process. The particle morphology and particle size were similar to those of $\text{Ca}_7\text{ZrAl}_6\text{O}_{18}$ (Fig. 3(D)), and the specific surface area increased from 0.8 to 1.4 m^2/g after milling.

3.2. Hydration

$\text{Ca}_7\text{ZrAl}_6\text{O}_{18}$ immediately reacted with water after mixing. The XRD pattern of the paste hydrated for 10 min (directly synthesized

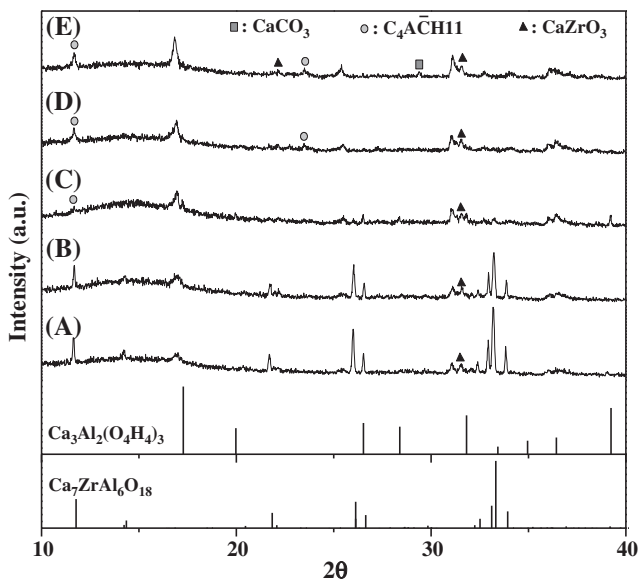


Fig. 4. XRD patterns of hydrated $\text{Ca}_7\text{ZrAl}_6\text{O}_{18}$ synthesized by polymeric precursor process as a function of hydration time; (A) 10 min, (B) 1 h, (C) 1 day, (D) 3 days, and (E) 7 days.

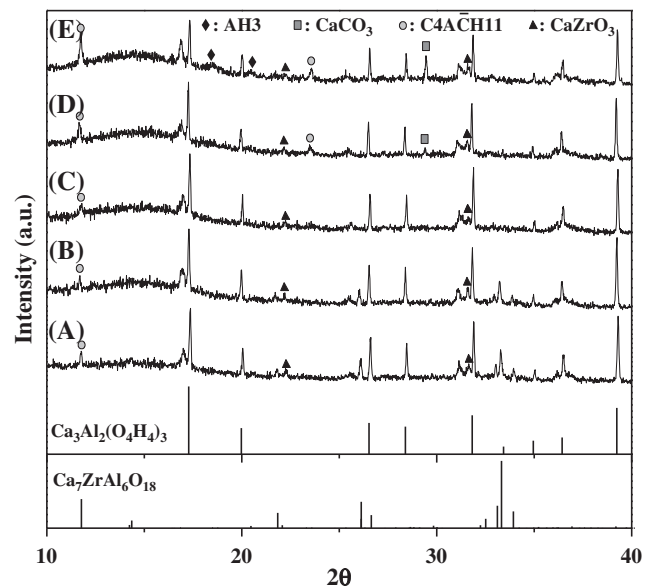


Fig. 5. XRD patterns of hydrated $\text{Ca}_7\text{ZrAl}_6\text{O}_{18}$ synthesized by polymeric precursor process and planetary ball milling as a function of hydration time; (A) 10 min, (B) 1 h, (C) 1 day, (D) 3 days, and (E) 7 days.

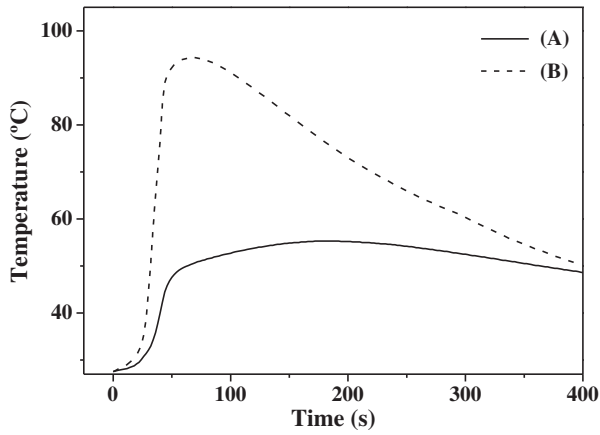


Fig. 6. Temperature rise during hydration of $\text{Ca}_7\text{ZrAl}_6\text{O}_{18}$. Both cements were prepared by polymeric precursor process at 1200 °C. Sample (B) was planetary ball milled.

$\text{Ca}_7\text{ZrAl}_6\text{O}_{18}$ by polymeric precursor method) showed the weak diffraction peaks for hydration products (Fig. 4(A)). The peak intensity for hydration products increased with the curing time, and after 1 day, $\text{Ca}_7\text{ZrAl}_6\text{O}_{18}$ phase almost disappeared (Fig. 4(C)). Further increase of curing time to 7 days resulted in the increase of peak intensity for hydration products without the phase change (Fig. 4(D), (E)). The CaZrO_3 phase was still present in the hydrates up to 7 days. The hydrates of $\text{Ca}_7\text{ZrAl}_6\text{O}_{18}$ were different from that of C3A. When the hydration of C3A occurs, $\text{Ca}_3\text{Al}_2\text{O}_6 \cdot 6\text{H}_2\text{O}$ (C3AH6) was readily formed, but C3A still remained up to 7 days (not shown here). In the diffraction patterns of $\text{Ca}_7\text{ZrAl}_6\text{O}_{18}$ hydrates, CaCO_3 and C4ACH11 ($4\text{CaO} \cdot \text{Al}_2\text{O}_3 \cdot \text{CO}_2 \cdot 11\text{H}_2\text{O}$) phases were identified. The rest of the un-indexed peaks were weak and broad and could be indexed to be $2\text{CaO} \cdot \text{Al}_2\text{O}_3 \cdot 8\text{H}_2\text{O}$ (C2AH8), $4\text{CaO} \cdot \text{Al}_2\text{O}_3 \cdot 19\text{H}_2\text{O}$ (C4AH19), $\text{Ca}_2\text{Al}(\text{OH})_7 \cdot 3\text{H}_2\text{O}$ (C4AH13), and $3\text{CaO} \cdot \text{Al}_2\text{O}_3 \cdot \text{Ca}(\text{OH})_2 \cdot 18\text{H}_2\text{O}$ [19–21]. To confirm the hydration products of $\text{Ca}_7\text{ZrAl}_6\text{O}_{18}$, TG-DTA and FT-IR analyses were additionally performed (see the Supplementary data Figs. S2 and S3 and Tables S1

and S2). Based on the obtained results and previous report [10], C2AH8, C4AH19, and C4AH13 were finally identified as hydration products of $\text{Ca}_7\text{ZrAl}_6\text{O}_{18}$ along with CaCO_3 and C4ACH11. These phases are known to be the metastable intermediate hydration products of calcium aluminate cements, which eventually convert to C3AH6 [21]. However, the intermediate phases were still found in the paste hydrated for 28 days and C3AH6 was not detected. It is speculated that the presence of Zr (or ZrO_2) stabilizes the intermediate hydration products. The $\text{Ca}_7\text{ZrAl}_6\text{O}_{18}$ powder prepared by solid state reaction exhibited the similar hydration behavior. On the other hand, the different hydration products were found in the paste of $\text{Ca}_7\text{ZrAl}_6\text{O}_{18}$ prepared through planetary ball milling as shown in Fig. 5. Both C3AH6 and intermediate phases were immediately formed (Fig. 5(A)) and they continued to exist up to 7 days (Fig. 5(B)–(F)). The peak intensity was almost unchanged with curing time and no conversion from intermediate phases to C3AH6 was observed. The peaks for $\text{Ca}_7\text{ZrAl}_6\text{O}_{18}$ were not found in the pastes hydrated for more than 1 day similar to the directed synthesized $\text{Ca}_7\text{ZrAl}_6\text{O}_{18}$ (Fig. 4(C)). Consequently, the formation of C3AH6 during hydration of $\text{Ca}_7\text{ZrAl}_6\text{O}_{18}$ was strongly dependent on the particle size or surface area. To find out the origin for the different hydration products depending on the particle size, the temperature change at the early stage of hydration was monitored by inserting the conventional probe type digital thermometer in the pastes (Fig. 6). The temperature rise was faster and the maximum temperature was higher in the paste of $\text{Ca}_7\text{ZrAl}_6\text{O}_{18}$ prepared through planetary ball milling. It is known that the metastable C4AH19 and C2AH8 phases convert to C3AH6 when left in air or when heated [21,22]. Thus, the formation of C3AH6 in the paste of $\text{Ca}_7\text{ZrAl}_6\text{O}_{18}$ prepared through planetary ball milling can be attributed to the higher exothermic reaction or higher temperature rise.

The morphology of the pastes hydrated for 3 days are shown in Fig. 7. Only irregular flakes were observed in the paste of directed synthesized $\text{Ca}_7\text{ZrAl}_6\text{O}_{18}$ (Fig. 7(A)) and both irregular flakes and isotropic particles (octahedron-like) were found in the paste of $\text{Ca}_7\text{ZrAl}_6\text{O}_{18}$ prepared through planetary ball milling (Fig. 7(B)). The hydration products of C3A pastes had the isotropic morphology close to spherical shape

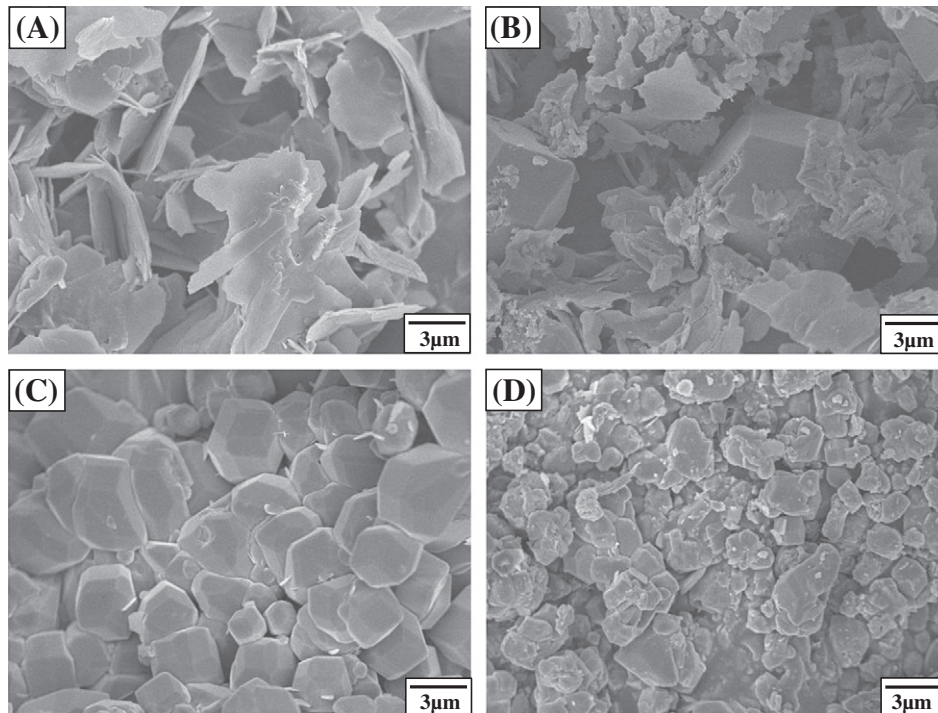


Fig. 7. FE-SEM micrographs of hydrated (A, B) $\text{Ca}_7\text{ZrAl}_6\text{O}_{18}$ and (C, D) C3A. All the cements were prepared by polymeric precursor process at 1200 °C and hydrated for 3 days. (B) and (D) were planetary ball milled cements.

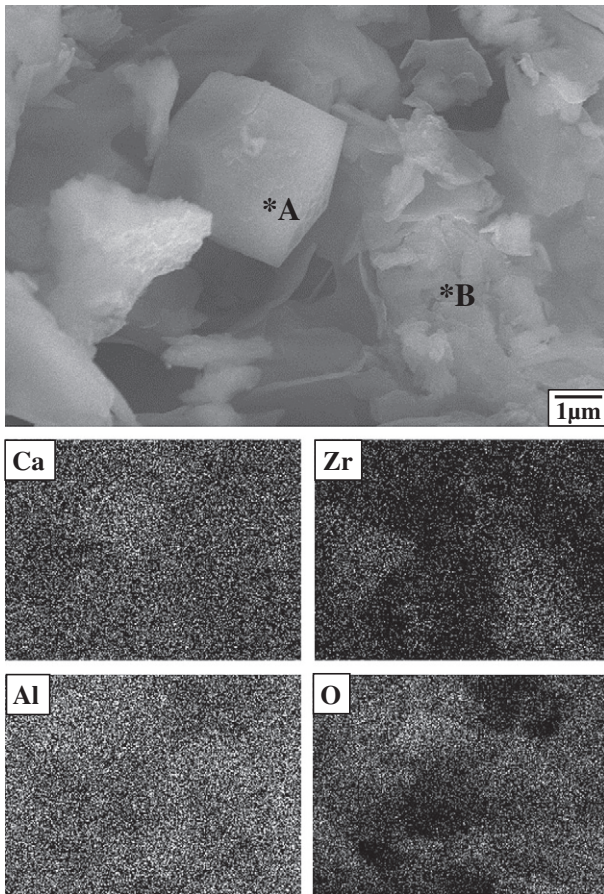


Fig. 8. FE-SEM image and EDS mapping of hydrated $\text{Ca}_7\text{ZrAl}_6\text{O}_{18}$ prepared by polymeric precursor process and planetary ball milling (3 day hydration).

(Fig. 7(C) and (D)). The intermediate phases, C4AH19 and C2AH8, commonly have the morphology of hexagonal flake or irregular flake, and the C3AH6 phase exhibits the isotropic or cubic morphology [19–21]. Thus, the observed morphology of $\text{Ca}_7\text{ZrAl}_6\text{O}_{18}$ pastes was consistent with the XRD results.

The elemental distribution in the hydrate of $\text{Ca}_7\text{ZrAl}_6\text{O}_{18}$ was examined by EDS (Fig. 8). The EDS mapping showed that Ca and Al were uniformly distributed, but Zr was rather locally present. The isotropic particle marked by “A” contained 1.2 at.% Zr whereas the irregular flake marked by “B” had 5.6 at.% Zr. Consequently, Zr was more concentrated in the intermediate hydration products, and the presence of Zr (or ZrO_2) retards or inhibit the transformation into the stable hydration product (C3AH6). Madej et al. reported that CaZrO_3 was separated from $\text{Ca}_7\text{ZrAl}_6\text{O}_{18}$ during hydration based on the increased intensity of CaZrO_3 peaks in the hydrated sample [10]. However, CaZrO_3 phase was not detected in the hydrates of single phase $\text{Ca}_7\text{ZrAl}_6\text{O}_{18}$ prepared in $\text{ZrO}(\text{NO}_3)_2 = 0.9$ condition (see the Supplementary data Fig. S4), which indicates that Zr is present in the hydration products instead of separating into CaZrO_3 phase.

The radiopacity of $\text{Ca}_3\text{Al}_2\text{O}_6$ and $\text{Ca}_7\text{ZrAl}_6\text{O}_{18}$ was evaluated by a standard X-ray machine, and the digital images of the radiographs are shown in Fig. 9. When calcium aluminate or calcium silicate is used as a root-end filling material, it needs to be discernible from dentin and root canal filling material. The International Organization for Standardization (ISO) 6876 specification for dental root canal sealing materials states that the radiopacity should be greater than a 3 mm thickness of aluminum [23]. The images indicate that 1 mm thickness of $\text{Ca}_7\text{ZrAl}_6\text{O}_{18}$ has a radio-opacity equivalent to not less than 3 mm of aluminum, and

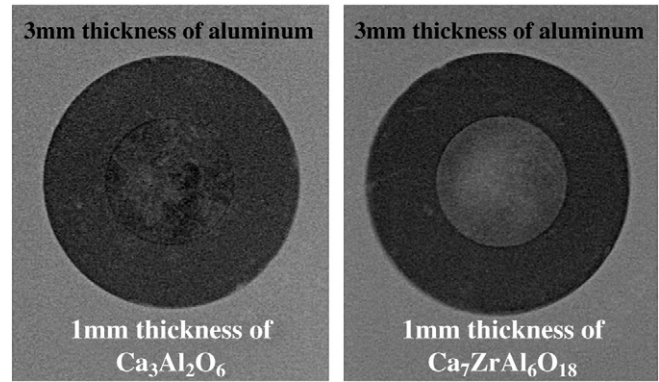


Fig. 9. Digital images of X-ray radiographs of C3A and $\text{Ca}_7\text{ZrAl}_6\text{O}_{18}$ cements hydrated for 28 days.

it shows a better radio-opacity than C3A. These preliminary results showed that $\text{Ca}_7\text{ZrAl}_6\text{O}_{18}$ has a potential for substituting the C3A phase in dentistry.

4. Conclusions

A nearly single phase $\text{Ca}_7\text{ZrAl}_6\text{O}_{18}$ was synthesized at relatively low temperature of 1200 °C through polymeric precursor process. The hydration behavior of $\text{Ca}_7\text{ZrAl}_6\text{O}_{18}$ was similar to that of C3A, but the hydration products were different. The intermediate hydration products of C3A persistently exist in the hydrates of $\text{Ca}_7\text{ZrAl}_6\text{O}_{18}$, which appears to be related to the degree of heat evolution, but further studies are required to find out the reason. The $\text{Ca}_7\text{ZrAl}_6\text{O}_{18}$ shows a better radiopacity than C3A and thus, $\text{Ca}_7\text{ZrAl}_6\text{O}_{18}$ cement is expected to be used as a dental root filling and/or repair material with a radiopacifier (ZrO_2).

Acknowledgments

This work was supported by the National Research Foundation of Korea (NRF) grant funded by the Korea government (MEST) (no. 2012-008226).

Appendix A. Supplementary data

Supplementary data to this article can be found online at <http://dx.doi.org/10.1016/j.cemconres.2013.11.007>.

References

- [1] J. Camilleri, M.G. Gandolfi, Evaluation of the radiopacity of calcium silicate cements containing different radiopacifiers, *Int. Endod. J.* 43 (2010) 21–30.
- [2] I. Islam, H.K. Chng, A.U. Yap, Comparison of the physical and mechanical properties of MTA and Portland cement, *J. Endod.* 32 (2006) 193–197.
- [3] E.-C. Kim, B.-C. Lee, H.-S. Chang, W. Lee, C.-U. Hong, K.-S. Min, Evaluation of the radiopacity and cytotoxicity of Portland cements containing bismuth oxide, *Oral Surg. Oral Med. Oral Pathol. Oral Radiol. Endod.* 105 (2008) e54–e57.
- [4] E. Saliba, S. Abbassi-Ghadi, R. Vowles, J. Camilleri, S. Hooper, J. Camilleri, Evaluation of the strength and radiopacity of Portland cement with varying additions of bismuth oxide, *Int. Endod. J.* 42 (2009) 322–328.
- [5] F.G. Aguilar, L.F.R. Garcia, H.L. Rossetto, L.C. Pardini, F.C.P. Pires-de-Souza, Radiopacity evaluation of calcium aluminate cement containing different radiopacifying agents, *J. Endod.* 37 (2011) 67–71.
- [6] M.A.H. Duarte, G.D. de Oliveira El Kadre, R.R. Vivan, J.M.G. Tanomaru, M.T. Filho, I.G. de Moraes, Radiopacity of Portland cement associated with different radiopacifying agents, *J. Endod.* 35 (2009) 737–740.
- [7] A.S. Bereznoi, R.A. Tarnopol'skaya, Calcium aluminozirconate – a new hydraulic binder, *Neorg. Mater. Akad. Nauk* 4 (1968) 2151–2154.
- [8] A.S. Bereznoi, R.A. Kordyuk, Melting diagram of the system $\text{CaO}-\text{Al}_2\text{O}_3-\text{ZrO}_2$, *Dopov. Akad. Nauk Ukr. RSR* 10 (1963) 1344–1347.
- [9] K. Fukuda, T. Iwata, K. Nishiyuki, Crystal structure, structural disorder, and hydration behavior of calcium zirconium aluminate, $\text{Ca}_7\text{ZrAl}_6\text{O}_{18}$, *Chem. Mater.* 19 (2007) 3726–3731.
- [10] D. Madej, J. Szczepka, W. Nocun'-Wczelik, R. Gajerski, Hydration of $\text{Ca}_7\text{ZrAl}_6\text{O}_{18}$ phase, *Ceram. Int.* 38 (2012) 3821–3827.

- [11] P.A. Lessing, Mixed-cation oxide powders via polymeric precursors, *Am. Ceram. Soc. Bull.* 68 (1989) 1002–1007.
- [12] M.P. Pechini, US Patent # 3,330,697 (1967).
- [13] A. Gaki, R. Chrysafi, G. Kakali, Chemical synthesis of hydraulic calcium aluminate compounds using the Pechini technique, *J. Eur. Ceram. Soc.* 27 (2007) 1781–1784.
- [14] S.-H. Hong, J.F. Young, Hydration kinetics and phase stability of dicalcium silicate synthesized by the Pechini process, *J. Am. Ceram. Soc.* 82 (1999) 1681–1686.
- [15] Y.M. Kim, S.-H. Hong, Influence of minor ions on the stability and hydration rates of β -dicalcium silicate, *J. Am. Ceram. Soc.* 87 (2004) 900–905.
- [16] V.D. Barbanyagre, D.A. Mishin, Synthesis and some properties of a new compound in the $\text{CaO}-\text{Al}_2\text{O}_3-\text{ZrO}_2$ system, *Refract. Ind. Ceram.* 41 (2000) 356–359.
- [17] Y.-L. Chai, Y.-S. Chang, G.-J. Chen, Y.-J. Hsiao, The effects of heat-treatment on the structure evolution and crystallinity of ZnTiO_3 nano-crystals prepared by Pechini process, *Mater. Res. Bull.* 43 (2008) 1066–1073.
- [18] Y.-S. Chang, F.-M. Huang, Y.-Y. Tsai, L.-G. Teoh, Synthesis and photoluminescent properties of $\text{YVO}_4:\text{Eu}^{3+}$ nano-crystal phosphor prepared by Pechini process, *J. Lumin.* 129 (2009) 1181–1185.
- [19] E. Breval, Gas-phase and liquid-phase hydration of C3A, *Cem. Concr. Res.* 7 (1977) 297–304.
- [20] E. Breval, C₃A hydration, *Cem. Concr. Res.* 6 (1976) 129–138.
- [21] A.-K. Maier, L. Dezmirean, J. Will, P. Greil, Three-dimensional printing of flash-setting calcium aluminate cement, *J. Mater. Sci.* 46 (2011) 2947–2954.
- [22] A.C. Jupe, X. Turrillas, P. Barnes, S.L. Colston, C. Hall, D. Hausermann, M. Hanfland, Fast in situ X-ray-diffraction studies of chemical reactions: a synchrotron view of the hydration of tricalcium aluminate, *Phys. Rev. B* 53 (1996) R14697–R14700.
- [23] International Organization for Standardization, Specification for Dental Root Canal Sealing Materials, ISO 6876, British Standards Institution, London, 1986. 1–4.